

## Phase state diagrams of the poly(dimethylsiloxane)—poly(diethylsiloxane) system

*E. M. Chaika,<sup>a\*</sup> A. E. Chalykh,<sup>b</sup> V. K. Gerasimov,<sup>b</sup> and V. S. Papkov<sup>a</sup>*

<sup>a</sup>*A. N. Nesmeyanov Institute of Organoelement Compounds, Russian Academy of Sciences,  
28 ul. Vavilova, 119991 Moscow, Russian Federation.*

*Fax: +7 (095) 135 5085. E-mail: chaika@ineos.ac.ru*

<sup>b</sup>*Institute of Physical Chemistry, Russian Academy of Sciences,  
31 Leninsky prosp., 119991 Moscow, Russian Federation.*

*Fax: +7 (095) 952 5308. E-mail: vladger@mail.ru*

Phase equilibria in the poly(dimethylsiloxane)(PDMS)—polydiethylsiloxane (PDES) system in the amorphous and liquid-crystal states were studied by optical interferometry. The findings obtained were compared with the data of calorimetric measurements. The experiments were carried out in a wide range of molecular weights and temperatures, and the phase diagrams were constructed. Thermodynamic analysis of the experimental data was performed in the framework of the Flory—Huggins theory for polymeric solutions. The analytical expressions for calculation of the pair interaction parameter using the binodal and liquidus curves were obtained. The pair interaction parameters of polymers and their dependences on the temperature and molecular weight were determined. The pair interaction parameter was shown to decrease with increasing the molecular weight of the oligomer component, approaching asymptotically a limiting value, which characterizes the interaction of the high molecular-weight PDMS and PDES. It was shown that the phase equilibria in the PDMS—PDES systems can be predicted quantitatively and qualitatively.

**Key words:** polydimethylsiloxane, polydiethylsiloxane, phase equilibria, temperature of phase separation, isotropization temperature, interaction parameter.

Polymer mixing is one of the efficient methods for preparation of composite polymeric materials, rubbers, and thermo- and reactoplastics. A number of scientific and engineering problems of polymer mixing have been elucidated in detail in the literature.<sup>1–3</sup> Organoelement polymer blends, in particular those of such important class of polymers as polyorganosiloxanes, have been studied to a lesser extent, at least in scientific sense. Among them, the blends of polydimethylsiloxane (PDMS) with polydiethylsiloxane (PDES) are of undoubted interest.

One can expect that polymeric materials for technics and medicine based on these blends will combine such well-known properties of PDMS as enhanced thermo- and frost-resistance, hydrophobicity, biocompatibility, and high thromboresistance<sup>4</sup> with specific mechanical properties of PDES, which is an example of mesomorphic elastomers.<sup>5,6</sup>

One of the key problems in the polymer blends area is the level of the thermodynamic compatibility of components, which determines the morphology and mechanical properties of the blend to a significant extent. In this work, the phase equilibria in the PDMS—PDES system in a wide range of the molecular weights (MW) of both com-

ponents are studied. Because of the low glass transition temperature and viscosity, the similarity of the chemical structure of both polymers, and the mesomorphic behavior of PDES, the PDMS—PDES compositions are the convenient model systems to study the general features of the polymer compatibility.

The work<sup>7</sup> in which the phase equilibria of PDMS—PDES were studied is the closest in its themes. However, the authors of work<sup>7</sup> did not go beyond the narrow range of MW of PDMS (up to 1000 g mol<sup>-1</sup>), and this did not allow the conclusions on the mutual solubility of high-molecular PDMS and PDES to be drawn.

The goal of this work is to study experimentally the phase equilibria in the PDMS—PDES systems in the wide range of temperatures and MW of both components.

### Experimental

We used a high-molecular PDMS (trade mark SKT), linear oligodimethylsiloxanes with terminal trimethylsiloxy groups (trade mark PMS);<sup>8</sup> PDES of a linear structure, which was obtained by KOH-induced polymerization of hexaethylcyclotrisiloxane,<sup>9</sup> and oligodiethylsiloxanes of predominantly linear

**Table 1.** Characteristics of studied polymers

Linear polysiloxanes	$M_n$	$M_w$	$\nu^{20*}$ /mm <sup>2</sup> s <sup>-1</sup>	$n_D^{20**}$
PDMS-1	—	$5.0 \cdot 10^5$	—	1.4071
PDMS-2	8100	—	500	1.4052
PDMS-3	5100—6400	—	200	1.4050
PDMS-4	2000—3000	—	50	1.4033
PDMS-5	950—1500	—	10	1.4013
PDES-1	$3.27 \cdot 10^5$	$7.27 \cdot 10^5$	$>10^6$	1.4536
PDES-2	7024	20588	—	1.4485
PDES-3	2593	4022	—	1.4478
PDES-4	—	900	44.3	1.4459

\* Kinematic viscosity at 20 °C.

\*\* Refraction index at 20 °C.

structure with terminal triethylsiloxy groups.<sup>8</sup> The characterization of the polymers is presented in Table 1.

The phase equilibria and processes occurring in the region of phase interface were studied by optical interferometry based on the appearance of an interference pattern in thin (~100 μm) films placed into a wedge-shaped gap between two semitransparent glasses.<sup>10</sup> The measurements were carried out with an ODA-2 optical diffusometer in the temperature range of 20–300 °C in the whole range of concentrations. The pure components PDMS and PDES interacted in the thermostatted cell, and as a result, the profile of the concentration distribution was established spontaneously in the region of the phase conjugation. This profile was due to the position of the figurative point of the system in the temperature–concentration field of the phase state diagram. The procedures of runs, the registration of interferograms, the construction of the concentration profiles, and the estimation of the compositions of the coexisting phases were described earlier.<sup>11</sup>

The refraction indices for polymers and their blends as functions of temperature were determined by preliminary experiments.<sup>12</sup> The measurements were performed on an Abbe refractometer (IRF-454BM) in the above-mentioned ranges of temperatures and compositions. Both the linear temperature dependences of the refraction index and the additive composition dependences of the refraction index were found for all components and their blends under study. Therefore, the obtained interferograms allowed us to evaluate the concentration profiles and their changes in time and upon the temperature variation.

## Results and Discussion

Typical interferograms of the zones of the mutual diffusion of the systems under study are shown in Fig. 1. One can observe continuous changes in the concentrations for the PDMS-1—PDES-4 system on going from one component to another (see Fig. 1, *a*). The facts that the interface is absent and the concentration profile is continuous indicate their complete compatibility in the whole temperature range studied.

The interferogram of the transition region of the phase interface in the PDMS-1—PDES-4 system obtained at the temperature above that of isotropization ( $T_i$ ) is a com-

bination of two zones of mutual diffusion (I and III) and the interface (II) (see Fig. 1, *b, d*). The phase boundary on the interferograms does not change its position in time, and the concentration jump at the interface remains constant and depends on only temperature, being reproducible in the heating–cooling cycles. Hence, the determined concentrations at the interface are equilibrium and correspond to the compositions of the coexisting phases.

The typical interferogram of the systems, which are characterized by a combination of the liquid-crystal equilibrium and amorphous phase separation, is presented in Fig. 1, *c*. In this case, the transition zone consists of three subzones: PDMS dissolution in mesomorphous PDES (I), PDMS solubility in the coexisting isotropic PDES phase (II), and PDES solubility in PDMS (III), as well as of two interfaces. With an increase in the MW of PDMS, its solubility in the amorphous PDES-1 phase decreases. This made it possible to suggest the one-side PDMS diffusion to the high-molecular PDES phase, unlike the systems containing cycloliner polysiloxanes and PDMS,<sup>13</sup> where the mutual diffusion takes place in the whole range of compositions. All above phase states are reproducible in the heating–cooling cycles, and this fact gives evidence of their equilibrium nature. The interferogram of the mutual diffusion zone formed upon cooling to temperature below  $T_i$  is exemplified in Fig. 1, *e*. One can see that the formation of the ordered regions of the liquid-crystal phase occurs in the phase enriched with PDES.

The state diagrams for the systems under study in the wide temperature–concentration field are shown in Figs. 2–4. The plots for the  $T_i$  depression vs. concentration obtained by the DSC method are presented in Fig. 4 (curve 3)<sup>7,14</sup> for comparison. As can be seen, all the systems studied are characterized by the upper critical temperature of phase separation (UCTS). The diagrams are asymmetrical as for the majority of polymeric systems with considerable differences in MW,<sup>15</sup> and the critical concentrations are shifted to the component with the lower MW. The data obtained are in good agreement with the phase diagram obtained previously.<sup>7</sup>

The effect of the MW of one of components on the compatibility of the systems under study is most pronounced in the isothermal sections of the phase state diagrams (Fig. 5). As can be seen, the experimental points typical of the PDES systems with MW =  $3.3 \cdot 10^5$  and of the PDMS systems with variable MW (see Fig. 5, *a*) are described by the straight lines in the  $\phi'(\phi'')-1/MW$  coordinates, where  $\phi'$ ,  $\phi''$  are the compositions of the coexisting phases. Under this representation of the binodal curves, the region of heterogeneous state is positioned between the straight lines and their intersection point is equivalent to the critical point at this temperature. Its position determines the maximal MW value below which the systems are completely compatible at given temperature. Similarly, suggesting analogous behavior of the blends

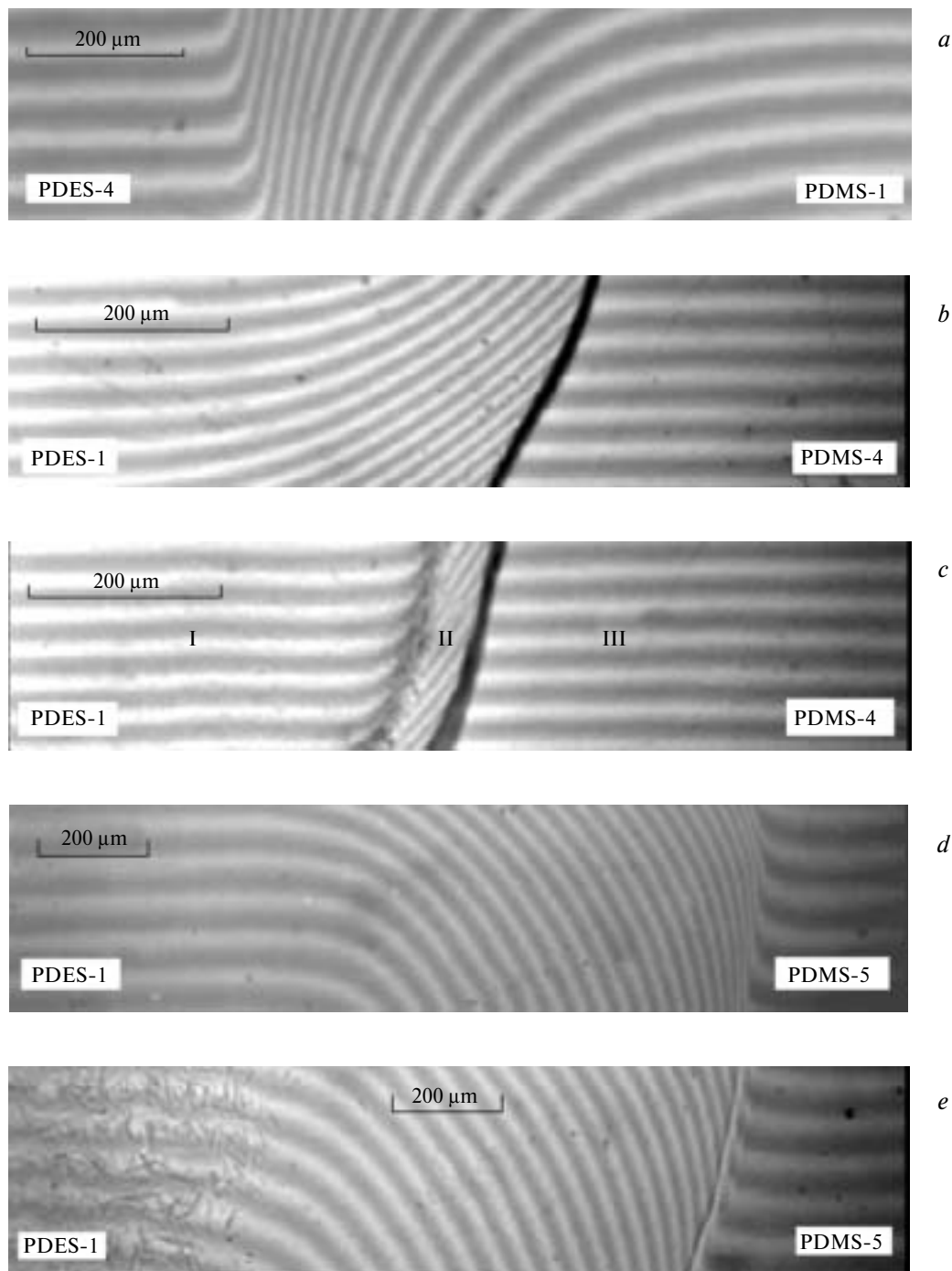


**Fig. 1.** Typical interferograms of PDES—PDMS systems: completely compatible (48 °C, 52 min) (a); amorphous phase separation at 62 °C, 161 min (b); combination of amorphous and liquid-crystal equilibria (33 °C, 77 min) (c); amorphous phase separation at 68 °C, 251 min (d); liquid-crystal equilibrium reached upon cooling (28 °C, 326 min) (e).

of high-molecular PDES with low-molecular PDMS and, conversely, the blends of high-molecular PDMS with the low-molecular PDES, the linear plot for the binodal concentrations vs. the MW of the low-molecular component for PDMS with  $MW = 5.0 \cdot 10^5$  and PDES with variable MW are presented in Fig. 5, *b*. As can be seen in Fig. 5,

the critical MW of low-molecular PDMS in a blend with high-molecular PDES is 1100 at 58 °C and 1500 at 150 °C. Note that the solubility depends on the ratio of MW and is independent of the nature of the high-molecular component within the limits of an experimental error. The findings obtained are in good agreement with the

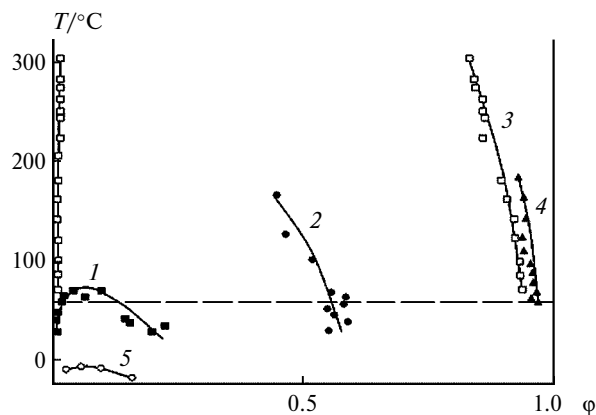


Fig. 2. Phase state diagrams of systems PDES-1—PDMS-5 (1), PDES-1—PDMS-4 (2), PDES-1—PDMS-3 (3), PDES-1—PDMS-2 (4), and PDES—PDMS-1000 (5)<sup>7</sup>,  $\phi$  is the PDES volume fraction. Dashed line designates  $T_g$  for PDES-1.

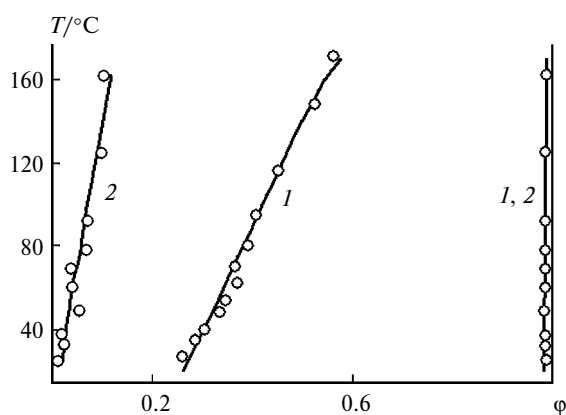


Fig. 3. Phase state diagrams of systems PDMS-1—PDES-3 (1) and PDMS-1—PDES-2 (2);  $\phi$  is the PDES volume fraction.

data of work<sup>7</sup> in which the upper critical temperature of mixing (UCTM) for the system PDES (MW =

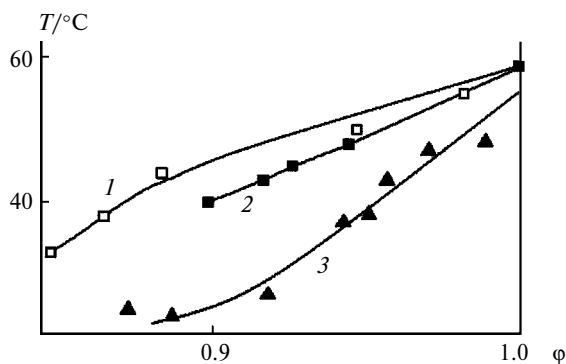


Fig. 4. Fragments of phase state diagrams (depression curves of isotropization temperature) of systems PDES-1—PDMS-4 (1), PDES-1—PDMS-5 (2) and PDES—PDMS-1000 (3)<sup>7</sup>;  $\phi$  is the PDES volume fraction.

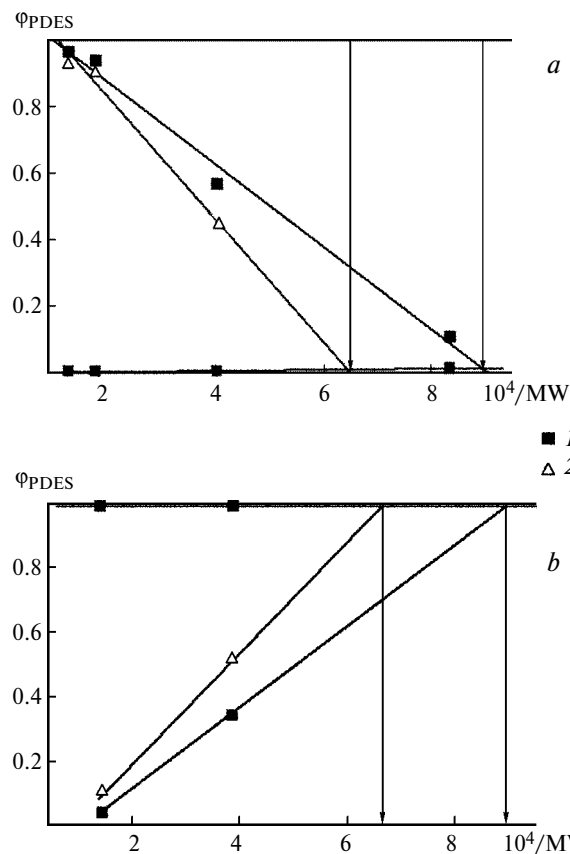


Fig. 5. Solubility of PDES-1 in PDMS with various MW (a) and of PDMS-1 in PDES with various MW (b) at 58 °C (1) and 150 °C (2).

$5.1 \cdot 10^5$ )—PDMS-1000 (MW = 1000) was found to be  $-4$  °C.

The depression  $T_i$  depends on the MW of PDMS (see Fig. 4), and the higher the MW of the amorphous component, the lower the depression. Similar data on the effect of the MW on depression  $T_i$  have been reported earlier.<sup>16</sup>

The swelling curves for the mesomorphic phase were measured for the PDES-1—PDMS-4 system, i.e., the PDMS solutions in mesomorphic PDES were found. As can be seen in Fig. 6, b, the degree of swelling decreases to zero with a decrease in temperature.

The thermodynamic analysis of the obtained experimental data on the phase equilibria of various types was performed with the use of the Flory—Huggins theory of polymeric solutions.

Remember that the condition for phase coexisting is the equality of the chemical potentials of components ( $\Delta\mu_i$ )

$$\Delta\mu'_i = \Delta\mu''_i \quad (1)$$

Here  $\Delta\mu'_i$ ,  $\Delta\mu''_i$  are the chemical potentials of the  $i$  component in the first and second phases, respectively. It is valid for both amorphous and liquid-crystal equilibria.

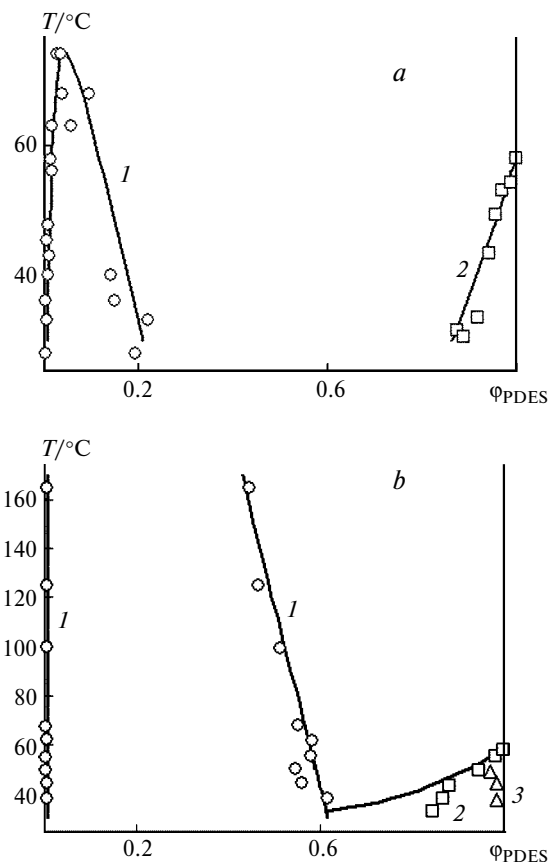


Fig. 6. Phase state diagrams of systems PDES-1-PDMS-5 (a) and PDES-1-PDMS-4 (b): binodal curve (1); depression of isotropization temperature (2); curves of swelling of the PDES amorphous phase (3). Solid lines designate the calculation data.

The expressions for the chemical potentials of the components upon the amorphous phase separation of the system are the following<sup>17</sup>:

$$\Delta\mu_1 = RT \left[ \frac{\ln \phi_1}{r_1} + \left( \frac{1}{r_1} - \frac{1}{r_2} \right) \phi_2 + \chi \phi_2^2 \right], \quad (2)$$

$$\Delta\mu_2 = RT \left[ \frac{\ln \phi_2}{r_2} + \left( \frac{1}{r_2} - \frac{1}{r_1} \right) \phi_1 + \chi \phi_1^2 \right]. \quad (3)$$

Here  $\phi_1$  and  $\phi_2$  are the concentrations of the first and second components, respectively;  $r_1$  and  $r_2$  are the degrees of polymerization of the first and second components, respectively, and  $\chi$  is the pair interaction parameter.

As applied to the amorphous phase separation, one can write

$$\begin{aligned} \frac{\ln \phi'_1}{r_1} + \left( \frac{1}{r_1} - \frac{1}{r_2} \right) \phi'_2 + \chi (\phi'_1)^2 &= \\ &= \frac{\ln \phi''_1}{r_1} + \left( \frac{1}{r_1} - \frac{1}{r_2} \right) \phi''_2 + \chi (\phi''_2)^2, \end{aligned} \quad (4)$$

$$\begin{aligned} \frac{\ln \phi'_2}{r_2} + \left( \frac{1}{r_2} - \frac{1}{r_1} \right) \phi'_1 + \chi (\phi'_1)^2 &= \\ &= \frac{\ln \phi''_2}{r_2} + \left( \frac{1}{r_2} - \frac{1}{r_1} \right) \phi''_1 + \chi (\phi''_1)^2. \end{aligned} \quad (5)$$

The joint solution of Eqs. (4) and (5) under the suggestion that  $\chi$  is independent of the concentration results in the expression

$$\chi = \frac{\ln(\phi''_1/\phi'_1)/r_1 - \ln(\phi''_2/\phi'_2)/r_2}{2(\phi'_2 - \phi''_2)}. \quad (6)$$

For temperatures below  $T_i$ , Eq. (1) acquires the form

$$\Delta\mu_2^{\text{meso}} = \Delta\mu_2^{\text{am}}, \quad (7)$$

$$\Delta\mu_1^{\text{sw}} = \Delta\mu_1^{\text{am}}, \quad (8)$$

where  $\Delta\mu_2^{\text{meso}}$  and  $\Delta\mu_2^{\text{am}}$  are the chemical potentials of PDES in the mesophase and in the coexisting amorphous phase, respectively;  $\Delta\mu_1^{\text{am}}$  and  $\Delta\mu_1^{\text{sw}}$  are the chemical potential of PDMS in the amorphous phase and in the coexisting swollen PDES phase.

The chemical potential<sup>14</sup> of the mesomorphic component in the liquid-crystal state is

$$\Delta\mu^{\text{meso}} = -\Delta H_{\text{meso}}(1 - T_i/T_i^{\circ}), \quad (9)$$

where  $T_i^{\circ}$  is the equilibrium isotropization temperature for the pure mesomorphic component,  $T_i$  is the equilibrium isotropization temperature for the mesomorphic component in the presence of the second isotropic or isomorphous component,  $\Delta H_{\text{meso}}$  is the enthalpy of isotropization. By substituting Eq. (9) and the expression for the chemical potential of PDES in the amorphous phase (3) into formula (7), we get

$$-\Delta H_{\text{meso}} \left( 1 - \frac{T_i}{T_i^{\circ}} \right) = RT_i \left[ \frac{\ln \phi_2}{r_2} + \left( \frac{1}{r_2} - \frac{1}{r_1} \right) \phi_1 + \chi \phi_1^2 \right]. \quad (10)$$

The solution of this equation with respect to  $\chi$  leads to the expression

$$\chi = \left[ \frac{-\Delta H_{\text{meso}}}{RT_i} \left( 1 - \frac{T_i}{T_i^{\circ}} \right) - \frac{\ln \phi_2}{r_2} - \left( \frac{1}{r_2} - \frac{1}{r_1} \right) \phi_1 \right] / \phi_1^2. \quad (11)$$

Under this approach, a change in  $T_i$  as a function of the composition of the solution is described as

$$T_i = 1 / \left\{ \frac{1}{T_i^{\circ}} - \frac{R}{\Delta H_{\text{meso}}} \left[ \frac{\ln \phi_2}{r_2} + \left( \frac{1}{r_2} - \frac{1}{r_1} \right) \phi_1 + \chi \phi_1^2 \right] \right\}. \quad (12)$$

We used expressions (6) and (11) for the analysis of the phase state diagrams for the amorphous and liquid-crystal equilibria.

The estimates of the pair interaction parameters from the binodal curves are presented in Figs. 7 and 8. As can

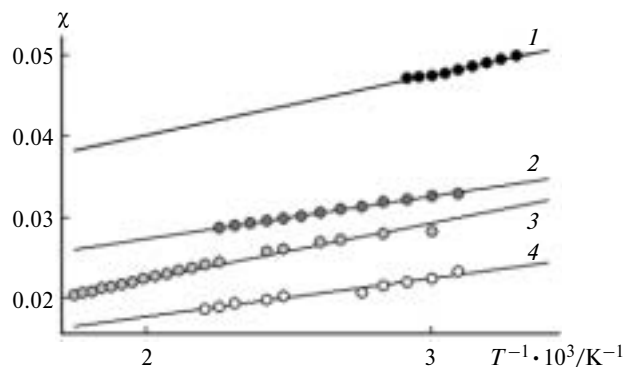


**Fig. 7.** The Haggins parameter ( $\chi$ ) vs. inverse temperature for systems PDES-1—PDMS-5 (1), PDES-1—PDMS-4 (2), PDES-1—PDMS-3 (3), and PDES-1—PDMS-2 (4).

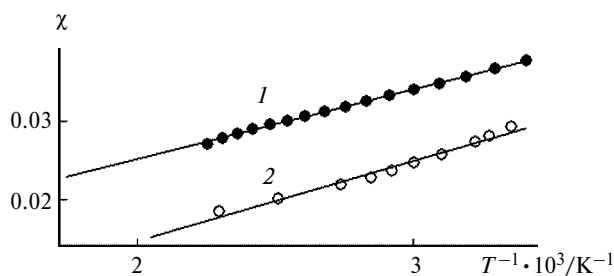


**Fig. 8.** The Haggins parameter ( $\chi$ ) vs. inverse temperature for systems PDMS-1—PDES-3 (1), PDMS-1—PDES-2 (2).

be seen, the linear dependence of the Haggins parameters on the inverse absolute temperature is observed for all the systems studied. With increasing the MW of the oligomeric component,  $\chi$  naturally decreases (Fig. 9), asymptotically reaching the limiting value  $\chi \approx 0.02$  at  $60^\circ\text{C}$ , which characterizes the interaction of two high-molecular PDMS and PDES. The interaction parameters for the solutions of high-molecular PDES in oligomeric PDMS and for the solutions of high-molecular PDMS in oligomeric PDES fall on the same curve and change by the same law.

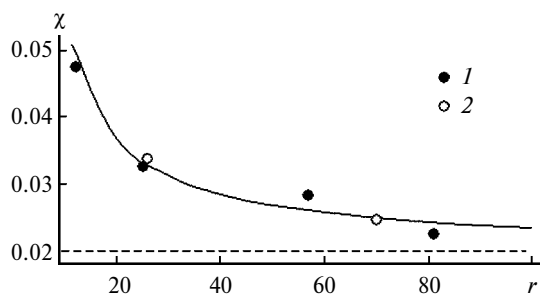


**Fig. 9.** The Haggins parameter ( $\chi$ ) vs. the degree of polymerization ( $r$ ) of low-molecular component for systems PDES-1 with PDMS of various MW (1) and PDMS-1 with PDES of various MW (2) at  $60^\circ\text{C}$ .

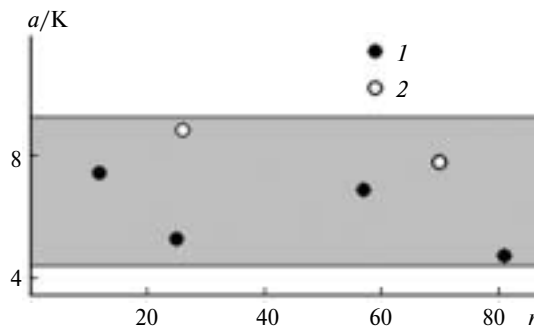


**Fig. 10.** Temperature coefficient of the enthalpy component of the Haggins parameter ( $a$ ) vs. degree of polymerization ( $r$ ) of low-molecular component for systems PDES-1 with PDMS of various MW (1) and PDMS-1 with PDES of various MW (2).

Note that all the  $\chi$  vs.  $1/T$  plots are characterized by the similar slope ratios. In the framework of the updated Flory—Haggins theory,<sup>18</sup> the slope of this dependence is connected with the enthalpy component of the pair interaction parameter ( $\chi_H$ ), i.e., it is proportional to the interaction energy for the segments of mixing polymers. The absolute term of the dependence  $\chi(1/T)$  characterizes the entropy component ( $\chi_S$ ).

Hence, the constancy of the temperature coefficient of the enthalpy component, which varies in the limited range  $6.8 \pm 2.0$ , confirms the suggestion that the segment interaction energy is independent of the MW (Fig. 10).

Unlike the temperature coefficient of the enthalpy component, the entropy component of the Haggins parameter (Fig. 11) is inversely proportional to the MW and the  $\chi_S$  value tends to zero at  $\text{MW} \rightarrow \infty$ . This means that the formation of nonideal solution upon mixing of two high-molecular components is due only to the enthalpy component.

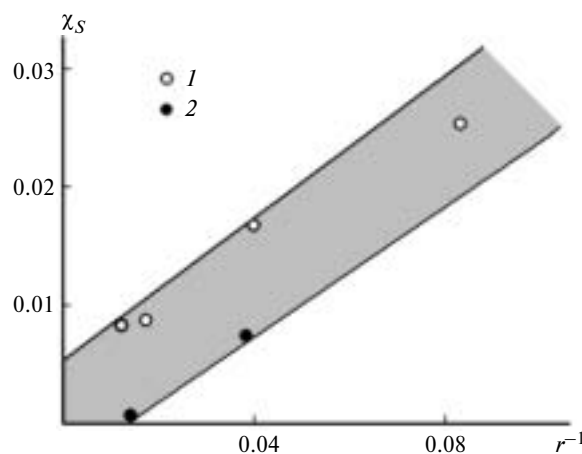


**Fig. 11.** Entropy component of the Haggins parameter ( $\chi_S$ ) vs. inverse degree of polymerization ( $r^{-1}$ ) of low-molecular component for systems PDES-1 with PDMS of various MW (1) and PDMS-1 with PDES of various MW (2).

On the basis of the data on the pair interaction parameters in the wide ranges of temperatures, compositions, and MW of the components, we attempted to construct the generalized phase state diagrams including both the amorphous and liquid-crystal equilibria. The calculations were carried out according to Eqs. (4), (5), and (12) by the extrapolation of the temperature dependence of the pair interaction parameter to the temperature region below  $T_i$ . The results of calculations are shown in Fig. 6. For comparison, the experimental compositions of the coexisting phases and the depressions  $T_i$  are listed in this figure. As can be seen, a satisfactory qualitative and quantitative agreement between the calculated and experimental data is observed. Note that in some systems, the experimental liquidus line is deviated from the calculated line to a greater extent. As we mentioned above,<sup>16</sup> this effect is due to the finite sizes of ordered regions and, as a consequence, the nonequilibrium experimental  $T_i$  values. More detailed analysis of the reasons for the discrepancy of the calculated and experimental values of both melting temperatures and  $T_i$  requires special investigation.

This work was supported by the Russian Foundation for Basic Research (Project Nos. 02-03-32186 and 02-03-32991).

### References

1. V. N. Kuleznev, *Smesi polimerov [Polymer Blends]*, Khimiya, Moscow, 1980, 304 pp. (in Russian).
2. *Polymer Blends*, Eds. D. R. Paul and S. Newman, Academic Press, New York, 1978, **1**; **2**.
3. *Multicomponent Polymer Systems*, Ed. R. F. Gould, Am. Chem. Soc., Washington, 1973.
4. I. M. Rabinovich, *Primenenie polimerov v meditsine [The Use of Polymers in Medicine]*, Meditsina, Leningrad, 1972, 198 pp. (in Russian).
5. V. S. Papkov, Yu. K. Godovskii, and V. S. Svistunov, *Vysokomol. Soedin., Ser. A*, 1989, **31**, 1577 [*Polym. Sci. USSR, Ser. A*, 1989, **31** (Engl. Transl.)].
6. V. Papkov, A. Turetsky, G. J. Out, and M. Moeller, *Int. J. Polym. Mat.*, 2002, **51**, 369.
7. T. M. Radzhabov, Yu. D. Shibanov, and Yu. K. Godovskii, *Vysokomol. Soedin., Ser. A*, 1988, **30**, 1667 [*Polym. Sci. USSR, Ser. A*, 1988, **30** (Engl. Transl.)].
8. *Oligoorganosiloksany. Svoistva, poluchenie, primeneniye [Oligoorganosiloxanes. Properties, Synthesis, and Application]*, Ed. M. V. Sobolevskii, Khimiya, Moscow, 1985, 264 pp. (in Russian).
9. V. S. Papkov, Yu. K. Godovsky, V. S. Svistunov, V. M. Litvinov, and A. A. Zhdanov, *J. Polym. Sci., Polym. Chem.*, 1984, **22**, 3617.
10. A. Ya. Malkin and A. E. Chalykh, *Diffuziya i vyazkost' polimerov. Metody izmereniya [Diffusion and Viscosity of Polymers. Measurement Techniques]*, Khimiya, Moscow, 1979, 304 pp. (in Russian).
11. A. E. Chalykh, A. I. Zagaitov, V. V. Gromov, and D. P. Korotchenko, *Opticheskii diffuziometr ODA-2 [Optical Diffusometer ODA-2]*, Institute of Physical Chemistry, Russian Academy of Sciences, Moscow, 1996, 36 pp. (in Russian).
12. A. E. Chalykh, A. Avgonov, E. M. Chaika, V. K. Gerasimov, V. S. Papkov, A. Yu. Rabkina, and B. G. Zavin, *Vysokomol. Soedin., Ser. A*, 2002, **44**, 1771 [*Polym. Sci., Ser. A*, 2002, **44**, No. 10 (Engl. Transl.)].
13. F. A. Avgonova, Ph. D. Thesis (Fiz. Math.), Institute of Physical Chemistry, Russian Academy of Sciences, Moscow, 2000, 144 pp. (in Russian).
14. T. M. Radzhabov, Ph. D. Thesis (Fiz. Math.), L. Ya. Karpov Research Institute for Physical Chemistry, Moscow, 1990, 150 pp. (in Russian).
15. *Polymer Blends*, Eds. D. R. Paul and C. B. Bucknall, Wiley, New York, 2000, 599 pp.
16. V. K. Gerasimov, A. E. Chalykh, and A. Avgonov, *Vysokomol. Soedin., Ser. A*, 2003, **45**, 409 [*Polym. Sci., Ser. A*, 2003, **45**, No. 3 (Engl. Transl.)].
17. P. J. Flory, *Principles of Polymer Chemistry*, Cornell Univ. Press, New York, 1953, 594 pp.
18. V. I. Klenin, *Termodinamika sistem s gibkotsepnymi polimerami [Thermodynamics of Systems of Flexible-chain Polymers]*, Izd-vo SGU, Saratov, 1995, 734 pp. (in Russian).

Received October 24, 2002;  
in revised form February 3, 2003